Bulletin of the Seismological Society of America, Vol. 92, No. 2, pp. 863–870, March 2002

Nonlinearity at California Generic Soil Sites from Modeling Recent Strong-Motion Data

by Igor A. Beresnev

Abstract The average strong- to weak-motion amplification ratios during the 1989 Loma Prieta and 1987 Whittier Narrows earthquakes in California are estimated by modeling strong ground motions at soil sites in the linear-response assumption and comparing the simulated and observed records. The linear amplification function, used to synthesize ground motions, is the generic transfer function developed for California soil. The database consists of 22 and 80 soil stations for the Loma Prieta and Whittier Narrows events, respectively. A statistically significant (at 95% confidence) reduction in amplification for the Loma Prieta event, within 40 km from the fault, is observed between approximately 1 and 3 Hz. Examining individual strong- to weak-motion amplifications as a function of peak acceleration at the base of soil, within this frequency range, shows that detectable reduction in amplification occurs at accelerations above about 200 cm/sec^2. The strong-motion amplification is reduced by a factor of 1.7–2 on average, relative to a generic weak-motion response. The results of this study suggest the magnitude of the reduction in amplification, caused by soil nonlinearity at large strain, that can be expected on average at California soil sites.

Introduction

The *M* 6.7, January 1994, Northridge, California, earthquake stimulated active research on the extent of nonlinear soil behavior at surrounding soil sites at high levels of strain (Field *et al.,* 1997; Beresnev *et al.,* 1998a,b; Field *et al.,* 1998; Hartzell, 1998; Su *et al.,* 1998; Cultrera *et al.,* 1999). This research was facilitated by the fact that a large collection of aftershock data had been obtained at many of the permanent strong-motion stations due to a rapid deployment of portable instruments after the mainshock. The Northridge aftershock database allowed calculation of site-specific weak-motion responses at the sites that also recorded strong ground motions with accelerations exceeding several hundred cm/sec^2. As a result, accurate responses at the same soil sites to both weak and strong motions could have been compared, with implications for ground nonlinearity.

For the other large California events, conducting a similar study would generally not be possible due to a lack of weak-motion records at the stations that recorded the mainshocks. Quantifying nonlinear amplification during those events would still be an important task, providing further observational constraints on the magnitude of nonlinear site response to be accounted for in hazard calculations. A possible solution to this problem could lie in the fact that most of California permanent strong-motion stations had been assigned one of the generic soil types and that generic amplification curves had been developed for each of these classes. The class-specific amplifications could then be substituted for site-specific responses, and one could check for consistency between amplifications based on the linearity assumption and those realistically observed during strong motions. Such an analysis will provide generic characteristics of nonlinearity, valid for the soil sites on average. This information is still of substantial interest to hazard assessment, since generic (class-specific) amplifications are typically used in developing detailed seismic-hazard maps for large urban areas (e.g., Building Seismic Safety Council, 1997; Petersen *et al.,* 1997). A check on nonlinearity in ground-motion amplification in California using generic, soil-class-based linear amplification functions is the goal of this study. Note that the previous studies for the Northridge event (Field *et al.,* 1997; Beresnev *et al.,* 1998a,b; Field *et al.,* 1998) used site-specific amplification functions, whose calculations had been made possible by the availability of large database of aftershock records recorded at the same locations. The Northridge earthquake was unique in this respect; for the other events, such information is not available, which necessitated the approach used in this article.

Method

In studying the characteristics of nonlinear amplification, we follow the approach taken by Beresnev *et al.*

(1998a). In this method, the finite-fault ground-motion prediction technique is first calibrated on rock sites to achieve a zero average prediction bias. The calibrated model is then applied to simulating recorded soil motions, with the only difference that the generated base motions (rock synth) are multiplied by the linear soil amplification function (lin amp), which is taken in the form of a generic amplification curve for a given site class. The generic curves are used because the site-specific amplifications are not available (no aftershock or small-event data have been recorded at the locations of strong-motion stations). The observed response spectrum (soil rec) is then divided by the predicted one (soil synth); if this ratio, averaged over all soil stations, falls below unity in a statistical sense, then the linear amplification has overestimated the real amplification, which is assumed to have been reduced by strain-dependent damping in soil. Before averaging, each ratio is normalized by the mean prediction bias for rock sites ($\langle$rock rec/rock synth$\rangle$) (which is close to unity), which removes the residual calibration error from soil-site simulations.

The described procedure can be represented as $\langle$(soil rec/soil synth)/$\langle$rock rec/rock synth$\rangle\rangle$, where the angular brackets denote station averaging. Since soil synth = lin amp $\times$ rock synth and soil rec = nonlin amp $\times$ rock rec, we can rewrite this expression as

$$\left\langle \frac{\text{nonlin amp}}{\text{lin amp}} \times \frac{\frac{\text{rock rec}}{\text{rock synth}}}{\left\langle \frac{\text{rock rec}}{\text{rock synth}} \right\rangle} \right\rangle \approx \left\langle \frac{\text{nonlin amp}}{\text{lin amp}} \right\rangle, \qquad (1)$$

where we have used the fact that the second factor under the large brackets oscillates around unity. The adopted procedure is thus equivalent to evaluating the average ratio of amplifications in strong and weak motions, with an estimate of its total uncertainty. The advantage of using the forward-modeling approach for estimating the amplification ratio is that the source and path effects have already been incorporated into the calibrated rock-motion simulation model, so that equation (1) effectively isolates the average ratio of site responses.

Averaging the ratio of the observed to predicted response spectra over all sites does not allow us to determine which particular soil stations primarily contributed to a possible nonlinear effect. To see whether these are the stations with the largest amplitudes of motions, which should be the case if the effect is caused by soil nonlinearity, we also plot individual ratios as a function of peak acceleration at the base of soil. This also gives us the way to estimate at which level of input motions the reduction in amplification becomes significant and serves as an independent check on whether this effect has been caused by nonlinearity and not some other factor.

The computer code FINSIM (Beresnev and Atkinson, 1998) was used in this study to generate the predicted response spectra at both rock and soil sites. The copies of all input and output files, along with a copy of the code, are freely available from the authors.

Data

We base our data selection for modeling on the response spectral database compiled by Pacific Engineering and Analysis (courtesy of W. J. Silva). Two California events—the *M* 6.1, October 1987, Whittier Narrows, and *M* 7.0, October 1989, Loma Prieta—provided the largest number of recordings at soil sites (80 and 22, respectively); these events were thus selected for the analysis. The soil sites are those assigned categories C and D on the Geomatrix site classification scale. These sites are categorized as generic soil, as opposed to the classes A and B that represent generic rock. The response spectra in the database are tabulated at frequencies equally spaced on a logarithmic scale (0.10, 0.14, 0.20, 0.28, 0.40, 0.56, 0.79, 1.12, 1.59, 2.24, 3.16, 4.47, 6.31, 8.92, and 12.6 Hz). The observed response spectral values at these frequencies are used in the analyses, except when certain values are flagged as unreliable by the creators of the database.

Figure 1 presents the linear amplification function for generic soil developed empirically from a large number of California soil profiles (Silva *et al.,* 1997). The transfer function was calculated relative to a generic-rock condition; this function was used in our simulations to amplify the synthetic rock motions. Tables 1–3 provide detailed information about the seismic events and soil stations that recorded strong ground motions. Most of the stations belong to class D.

Note that the use of a generic amplification curve for varying soil conditions adds to the uncertainty in modeling site-specific ground motions, since local amplification may differ from the generic curve. It should be remembered that the generic curves represent correct amplifications on aver-

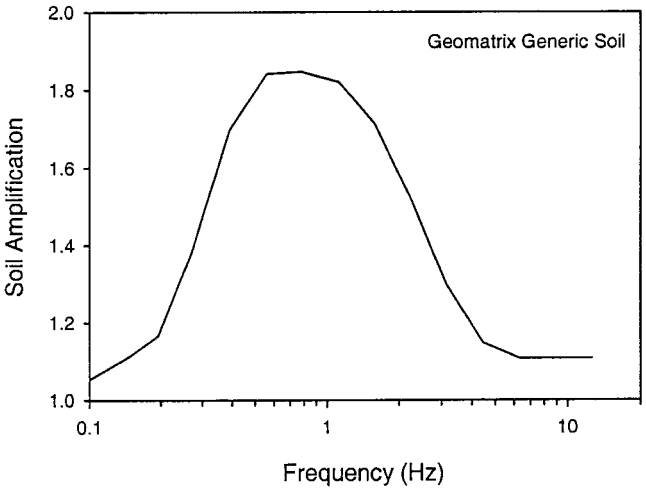

Figure 1. Mean linear transfer function for Geomatrix generic soil (classes C and D) relative to generic rock (classes A and B) (after Silva *et al.,* 1997).

Table 1
Characteristics of Events

Event	Moment Magnitude	Date (dd/mm/yy)	Epicenter Latitude	Epicenter Longitude	Number of Soil Stations
Loma Prieta	7.0	10/17/89	37.200	−122.030	22
Whittier Narrows	6.1	10/01/87	34.098	−118.015	80

Table 2
Soil Stations for the Loma Prieta Event*

Station Code†	Latitude (°)	Longitude (°)	Distance from Fault Plane (km)	Location	Owner	Geomatrix Site Class‡
G02	36.982	121.556	12.7	Gilroy Array #2	CDMG	D
GOF	37.009	121.569	12.7	Gilroy–Historic Bldg.	CDMG	D
STG	37.255	122.031	13.0	Saratoga–Aloha Ave.	CDMG	D
WVC	37.262	122.009	13.7	Saratoga–W. Valley Coll.	CDMG	D
G03	36.987	121.536	14.4	Gilroy Array #3	CDMG	D
CAP	36.973	121.953	14.5	Capitola	CDMG	C
G04	37.005	121.522	16.1	Gilroy Array #4	CDMG	D
WAH	36.990	121.996	16.9	WAHO	UCSC	D
AND	37.166	121.628	21.4	Anderson Dam (Downstream)	USGS	D
CLD	37.214	121.551	22.3	Coyote Lake Dam (Downst)	CDMG	D
HDA	36.888	121.413	25.8	Hollister Diff. Array	USGS	D
AGW	37.398	121.952	28.2	Agnews State Hospital	CDMG	D
HCA	36.850	121.400	28.2	Hollister City Hall	USGS	D
HSP	36.848	121.397	28.8	Hollister–South and Pine	CDMG	D
SVL	37.402	122.024	28.8	Sunnyvale–Colton Ave	USGS	D
HVR	37.338	121.714	31.6	Halls Valley	CDMG	C
SAL	36.671	121.642	32.6	Salinas–John and Work	CDMG	D
PAE	37.453	122.112	36.1	Palo Alto–1900 Embarc.	CDMG	D
A02	37.52	122.25	47.9	APEEL 2–Redwood City	USGS	D
A2E	37.657	122.082	57.4	APEEL 2E Hayward Muir Sch	CDMG	D
HWB	37.67	122.086	58.9	Hayward–BART Sta	CDMG	D
SFO	37.622	122.398	64.4	SF Intern. Airport	CDMG	D

*Source: Pacific Engineering and Analysis strong-motion database. Stations are listed in the order of increasing distance from fault.
†Assigned by Pacific Engineering and Analysis.
‡C, deep narrow soil; D, deep broad soil.

age. This will be reflected in an increase in the statistical measures of uncertainty determined for the estimated ratio of nonlinear to linear amplification using equation (1).

Results

Calibrated Model

Beresnev and Atkinson (2001, 2002) recently calibrated the finite-fault simulation model, implemented in the code FINSIM, for 17 large California events; the procedure followed was similar to that of model calibration for eastern North America (Beresnev and Atkinson, 1999). The calibrated model achieves a near-zero mean bias for modeling rock-site motions for both Loma Prieta and Whittier Narrows events with 95% confidence. These event-specific calibrated models are applied to the simulation of soil sites in this study.

Figure 2 shows rock-station misfit, defined as the ratio between the observed and simulated response spectrum, for the Loma Prieta and Whittier Narrows events, as a function of distance from the fault. This checks for the distance bias in the model, which can affect the analysis of nonlinear-response characteristics, since nonlinearity mostly occurs close to the source. The misfits are shown for a representative frequency of 1.6 Hz. Figure 2 shows a rather irregular distribution of rock-station misfits around the unity for both events, with no distinct bias in the studied distance range (up to 70 km for the Loma Prieta earthquake and 50 km for the Whittier Narrows earthquake). The soil stations (Tables 2 and 3) all lie within these distance ranges.

Average Strong- to Weak-Motion Amplification Ratio

By dividing the observed and simulated response spectra and averaging over all soil sites, we can estimate the mean ratio of amplifications that occurred in strong and weak motions. Not all of the stations within a 70- or 50-km radius from the Loma Prieta and Whittier Narrows events, respectively, could contribute equally to a possible average

Table 3
Soil Stations for the Whittier Narrows Event*

Station Code†	Latitude (°)	Longitude (°)	Distance from Fault Plane (km)	Location	Owner	Geomatrix Site Class‡
FAI	34.093	118.018	9.8	El Monte–Fairview Ave.	USC	D
JAB	33.965	118.158	9.8	Bell Gardens–Jaboneria	USC	D
COM	33.99	117.942	10.5	Hacienda Heights–Colima	USC	C
VER	34.004	118.23	10.8	LA–E Vernon Ave	USC	D
CYP	34.088	118.222	11.4	LA–Cypress Ave	USC	C
FIG	34.111	118.189	11.4	LA–N Figueroa St	USC	C
RIM	34.026	117.918	11.9	La Puente–Rimgrove Ave	USC	D
CAM	34.13	118.036	12.2	Arcadia–Campus Dr	USC	D
WHD	34.02	118.053	12.3	Whittier–N. Dam upstream	USGS	D
ALH	34.07	118.15	13.2	Alhambra–Fremont School	CDMG	D
BRC	33.946	117.924	13.5	La Habra–Briarcliff	USC	C
OBR	34.037	118.178	13.9	LA–Obregon Park	CDMG	D
BAD	34.087	117.915	14.2	Covina–W Badillo	USC	D
FLT	34.115	118.244	14.4	LA–Fletcher Dr	USC	D
GR2	34.005	118.279	14.5	LA–S Grand Ave	USC	D
OLD	34.171	118.079	14.5	Pasadena–Old House Rd	USC	C
SMA	34.115	118.13	14.7	San Marino–SW Academy	CDMG	D
ATH	34.14	118.12	15.4	Pasadena–CIT Athenaeum	CDMG	D
BRI	34.150	118.170	15.5	Pasadena–CIT Bridge Lab	CDMG	D
BRN	34.150	118.170	15.5	Pasadena–Brown Gym	CDMG	D
CAL	34.150	118.170	15.5	Pasadena–CIT Calif Blvd	CDMG	D
IND	34.150	118.170	15.5	Pasadena–CIT Indust. Rel	CDMG	D
KEC	34.150	118.170	15.5	Pasadena–CIT Keck Lab	CDMG	D
LUR	34.150	118.170	15.5	Pasadena–CIT Lura St	CDMG	D
MUD	34.150	118.170	15.5	Pasadena–CIT Mudd Lab	CDMG	D
70S	33.976	118.289	16.3	LA–W 70th St	USC	D
WST	34.082	118.298	16.6	LA–N Westmoreland	USC	D
CAS	33.899	118.196	16.9	Compton–Castlegate St	USC	D
GRA	34.078	117.87	17.1	Covina–S Grand Ave	USC	C
NOR	33.917	118.067	17.2	Norwalk–Imp Hwy, S Grnd	USGS	D
KRE	34.150	118.170	17.4	Pasadena–CIT Kresge Lab	CDMG	D
ALT	34.177	118.096	17.5	Altadena–Eaton Canyon	CDMG	D
FLO	33.916	117.896	17.9	Brea–S Flower Ave	USC	D
OR2	33.881	118.176	18.3	LB–Orange Ave	USC	D
PAL	34.2	118.231	19.0	Glendale–Las Palmas	USC	C
SAT	34.046	118.355	20.8	LA–Saturn St	USC	D
DEL	33.846	118.099	20.9	Lakewood–Del Amo Blvd	USC	D
116	33.929	118.26	22.5	LA–116th St School	CDMG	D
NYA	34.238	118.253	22.7	La Crescenta–New York	USC	C
BRD	33.889	117.926	23.3	Brea Dam (Downstream)	USGS	D
BUE	34.168	118.332	23.7	Burbank–N Buena Vista	USC	D
BAL	33.817	117.951	24.4	Anaheim–W Ball Rd	USC	D
WAT	33.836	118.239	24.5	Carson–Water St	USC	D
OSA	33.897	118.346	25.1	Lawndale–Osage Ave	USC	D
HOL	34.09	118.339	25.2	LA–Hollywood Stor FF	CDMG	D
ING	33.905	118.279	25.2	Inglewood–Union Oil	CDMG	D
TUJ	34.286	118.225	25.5	Big Tujunga, Angeles Nat F	USC	C
CER	33.84	118.194	26.0	LB–R. Los Cerritos	CDMG	D
BLD	34.009	118.361	27.0	LA–Baldwin Hills	CDMG	D
MRP	34.288	118.881	27.1	Moorpark–Fire Sta	CDMG	D
MU2	34.127	118.405	27.2	Beverly Hills 12520 Mulhol	USC	C
GLE	34.269	118.303	27.5	Sunland–Mt Gleason Ave	USC	C
CEN	34.001	118.43	27.7	LA–Centinela St	USC	D
CAT	33.812	118.27	28.1	Carson–Catskill Ave	USC	D
CO2	34.146	118.413	28.7	Studio City–Coldwater Can	USC	D
PMN	34.056	117.748	28.8	Pomona–4th and Locust FF	CDMG	D
SAR	33.96	118.432	28.8	Playa Del Rey–Saran	USC	D
MAN	33.886	118.388	28.9	Manhattan Beach–Manhattan	USC	C
MUL	34.132	118.439	30.3	Beverly Hills–14145 Mulhol	USC	C

(continued)

Table 3
(Continued)

Station Code[†]	Latitude (°)	Longitude (°)	Distance from Fault Plane (km)	Location	Owner	Geomatrix Site Class[‡]
REC	33.778	118.133	30.5	LB–Recreation Park	CDMG	D
COL	34.194	118.411	30.8	N Hollywood–Coldwater Can	USC	C
CTS	34.062	118.417	31.3	LA–Century City CC South	CDMG	D
CTN	34.064	118.417	31.4	LA–Century City CC North	CDMG	D
TOR	33.823	118.356	31.4	Torrance–W 226th St	USC	E
RO3	34.221	118.421	32.6	Sun Valley–Roscoe Blvd	USC	D
RO2	34.222	118.442	33.0	Panorama City–Roscoe	USC	D
KAG	34.251	118.42	34.0	Pacoima Kagel Canyon	USC	D
HAR	33.754	118.2	34.2	LB–Harbor Admin FF	CDMG	D
EUC	33.719	117.938	35.0	Fountain Valley–Euclid	USC	D
SEA	33.736	118.269	35.7	Terminal Island–S Seaside	USC	D
LUC	33.74	118.335	37.7	Rancho Palos Verdes–Luconia	USC	C
FEA	33.869	117.709	38.6	Featherly Park–Maint	CDMG	C
SAY	34.306	118.438	38.6	Sylmar–Sayre St	USC	D
ARL	34.236	118.439	38.9	Arleta–Nordhoff Fire Sta	CDMG	D
STA	34.209	118.517	39.8	Northridge–Saticoy St	USC	D
HNT	33.662	117.997	42.8	Huntington Beach–Lake St	CDMG	D
CUC	34.104	117.574	44.3	Rancho Cucamonga–Law and J	CDMG	D
LOS	34.419	118.426	46.4	Canyon Country–W Lost Can	USC	D
TOP	34.212	118.605	47.4	Canoga Park–Topanga Can	USC	D
SYL	34.326	118.444	47.7	Sylmar–Olive View Med FF	CDMG	D

*Source: Pacific Engineering and Analysis strong-motion database. Stations are listed in the order of increasing distance from fault.

[†]Assigned by Pacific Engineering and Analysis.

[‡]C, deep narrow soil; D, deep broad soil; E, soft deep soil.

nonlinear response; stations being closest to the source likely provided the maximum contribution. Our tests showed that the strong- to weak-motion amplification ratio was not statistically different from unity unless we retained the stations within a certain radius from the source, which generally recorded the highest accelerations. For the Loma Prieta event, this minimum radius was approximately 40 km. Figure 3 shows the logarithm (base 10) of the amplification ratio for the Loma Prieta earthquake, averaged over all soil sites within the 40-km radius (solid line). The dashed line shows the limit of uncertainty in the upper boundary of the ratio, based on one-tailed t distribution at the 95% confidence level. We conclude that, with 95% confidence, the mean ratio deviated below unity from approximately 1 to 3 Hz, within the specified distance range. This is the frequency range where an observable nonlinear soil response had likely occurred during the Loma Prieta event. This range is consistent with the interval of 2–4 Hz, in which a similar observable decrease in strong-motion amplification compared to that in weak motions was reported by Field *et al.* (1997, their figure 3) for the Northridge earthquake. Chin and Aki (1991) also noted that their predicted peak ground accelerations, based on a linearity assumption, systematically overestimated the observed values within the radius of approximately 50 km from the epicenter of the Loma Prieta earthquake. This extent of nonlinear soil response is consistent with the results of our analyses.

We were not able to identify a significant difference between the mean ratio of strong- to weak-motion amplification and unity for the Whittier Narrows earthquake within any radius from the source. To provide a plausible explanation for this result, we again note that the generic amplification function in Figure 1 is the mean value, whereas every site-specific amplification would deviate from the mean. An uncertainty in approximating the individual amplifications by the mean is implicitly included in the confidence limit shown in Figure 3. The reason for our inability to identify the average reduction in amplification during the Whittier Narrows event could be that the effect was not sufficiently large to exceed the uncertainty level. A natural explanation for the weaker effect is also the smaller magnitude of the Whittier Narrows event. For example, the highest observed near-fault horizontal acceleration on rock reached $0.64g$ during the Loma Prieta mainshock, compared to $0.46g$ during the Whittier Narrows event.

Amplification Ratio as a Function of Peak Acceleration

We now turn to examining the ratios of strong- to weak-motion amplification at individual soil sites as a function of input acceleration level. If the average reduction in amplification seen between 1 and 3 Hz in Figure 3 is caused by nonlinear soil response, then this effect should exhibit dependence on the amplitude of input to the soil column. An

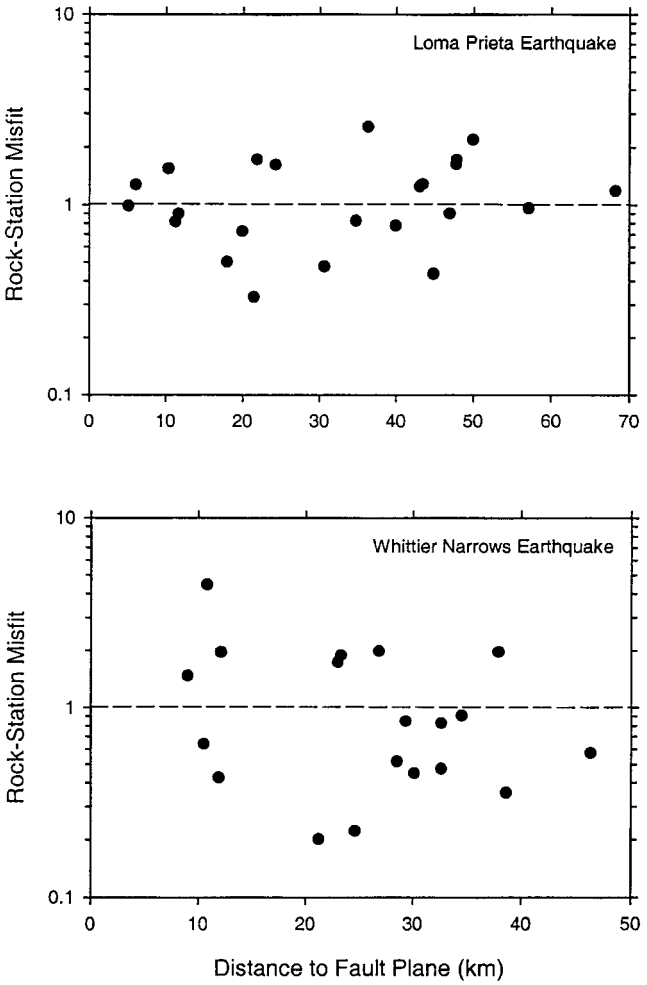

Figure 2. Misfit between the observed and simulated response spectral values at rock sites for the calibrated models of the Loma Prieta and Whittier Narrows earthquakes. Misfits are shown at 1.6 Hz.

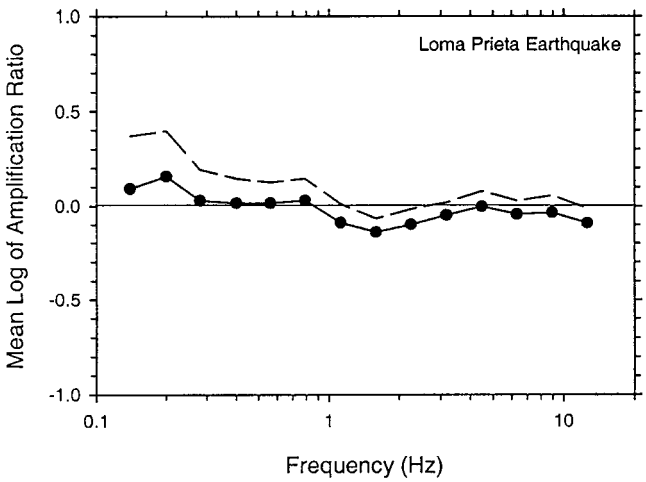

Figure 3. Mean strong- to weak-motion amplification ratio at the Loma Prieta soil sites within the radius of 40 km (solid line). Circles show the frequencies at which data have been obtained. The dashed line is the limit of uncertainty in the upper boundary of the ratio, at the 95% confidence level. A statistically significant deviation below unity occurs between 1 and 3 Hz, approximately.

existence of such dependence would confirm that the observed nonlinear response is real.

Figures 4 and 5 show individual strong- to weak-motion amplification ratios for the soil sites during the Loma Prieta and Whittier Narrows earthquakes, respectively, as a function of estimated peak horizontal acceleration at the base of soil. The estimates were obtained from the accelerograms generated by the calibrated code, with no site response applied; they were also corrected for the mean bias of rock-motion prediction at a corresponding frequency. The amplification ratios are plotted at 1.6 and 2.2 Hz, where observable nonlinear response was detected on average in Figure 3. Despite substantial scatter in the data, caused by both the uncertainty in the estimation of peak base acceleration and in the approximation of individual weak-motion amplifications by the mean, the data define a trend toward decreasing amplification with increasing input amplitude. This effect is seen at both frequencies. Figures 4 and 5 suggest that the strong-motion amplification becomes a factor of 0.5–0.6 of that in weak motions at the highest accelerations (i.e., a factor of 1.7–2.0 in amplification reduction). The effect becomes detectable roughly beyond 200–300 cm/sec^2 in Figure 4 and 200 cm/sec^2 in Figure 5. Both the magnitude of the amplification reduction and the acceleration range where it becomes observable are consistent with the results obtained for the Northridge earthquake. The amplification reduction by a factor of 2 was derived by Field *et al.* (1997, their figure 3), Beresnev *et al.* (1998a, their figure 4), and figure 10 of Su *et al.* (1998) (at the equivalent acceleration range). The acceleration level of 150–200 cm/sec^2, at which nonlinearity becomes significant, was obtained by Beresnev *et al.* (1998a, their figure 6).

Note that the scatter of data in both Figures 4 and 5 causes the value of amplification ratio to fall below unity even at low-acceleration levels. As mentioned previously, this scatter is caused by both uncertainties in representing the site-specific amplification functions by their generic values and in approximating the acceleration at the base of soil. Only the trend should be considered a significant feature of these data ensembles.

Discussion and Conclusions

Unlike the Northridge earthquake, the other recently recorded large seismic events in California have not generally provided a sufficient amount of weak-motion data at the sites of recorded strong motions to allow reliable comparison of site-specific amplifications at contrasting excitation levels. However, the average characteristics of amplitude-dependent amplification could still be assessed based on site-

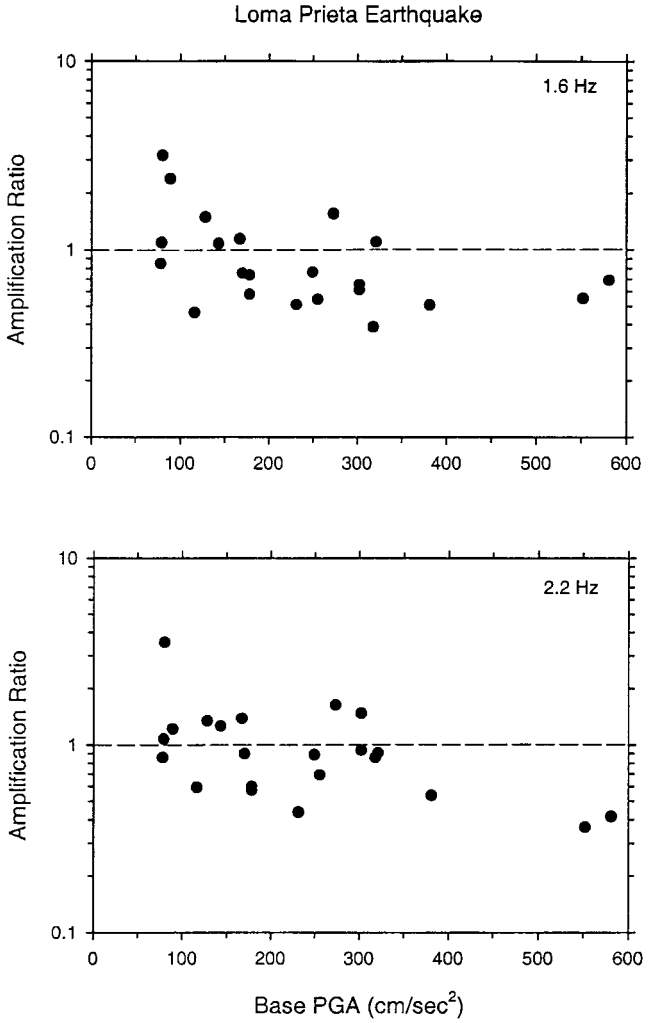

Figure 4. Individual strong- to weak-motion amplification ratios at soil sites during the Loma Prieta earthquake, as a function of estimated peak horizontal acceleration at the base of soil. Amplification ratios are shown at 1.6 and 2.2 Hz.

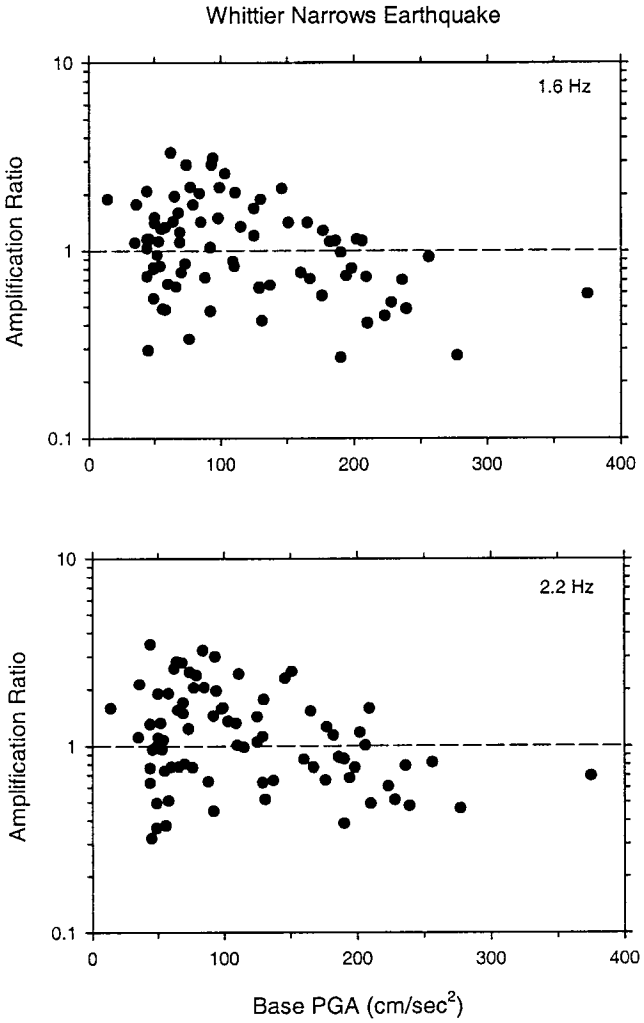

Figure 5. Individual strong- to weak-motion amplification ratios at soil sites during the Whittier Narrows earthquake, as a function of estimated peak horizontal acceleration at the base of soil. Amplification ratios are shown at 1.6 and 2.2 Hz.

classification information and amplification curves developed for the generic soil classes. This information is still of substantial interest to hazard analysis, which often deals with only crude characterization of site conditions (e.g., Field and SCEC Phase III Working Group, 2000).

The Loma Prieta and Whittier Narrows earthquakes are the recent events that provided the largest number of strong-motion records at soil sites (not counting the Northridge event, for which similar analyses using site-specific amplification functions were given by Beresnev *et al.,* 1998a). Our study estimated the strong- to weak-motion amplification factors during these events based on forward modeling of soil motions, assuming linear amplification, and comparison of the synthetics with the observed records.

The strong- to weak-motion amplification ratio, averaged over 22 soil sites for the Loma Prieta earthquake, showed a statistically significant reduction below unity in the frequency band from approximately 1 to 3 Hz. This is consistent with the result of Field *et al.* (1997) for the Northridge earthquake, obtained using an alternative site response–estimation technique. We were not able to identify a similar reduction in the average amplification for the Whittier Narrows event. A plausible explanation for this fact could be that significantly higher peak horizontal accelerations were developed in the epicentral area of the Loma Prieta event, causing stronger nonlinear effects. Also, the application of the generic amplification curve to a variety of site conditions increased the uncertainty in the estimation of the average amplification ratio; this may have prevented us from identifying the weaker effects during the Whittier Narrows event. The same reason may explain our inability to detect possible nonlinearity during the Loma Prieta earthquake above the frequencies of 1 to 3 Hz. For example, the studies of the differences in weak- and strong-motion am-

plification during the Northridge event, which were more accurate because site-specific weak-motion responses were available, have indicated that nonlinear reduction in amplification extended to approximately 10 Hz (Beresnev *et al.,* 1998a; Hartzell, 1998). We were not able to reach a similar conclusion for the Loma Prieta event. It remains to be seen whether nonlinearity at California soils typically extends to high frequencies of engineering significance or is limited to lower frequencies.

Examining individual amplification ratios as a function of input acceleration level shows that they exhibit a trend, despite large variability, toward a decrease below unity with increasing peak acceleration. The effect is seen beyond approximately 200 cm/sec^2 at the frequencies of 1.6 and 2.2 Hz. Figure 5 also suggests why we may not have been able to observe the average amplification-reduction effect for the Whittier Narrows event. It shows that most of the stations supplying the data were in fact in the linear range, overweighing the sites where nonlinear effect had likely occurred. As a result, averaging out all sites provided no significant deviation from unity. The Loma Prieta data extend to about 600 cm/sec^2, with a more uniform coverage of both low- and high-acceleration ranges, leading to an observable average nonlinear response.

From our study of generic nonlinear amplification characteristics, we conclude that nonlinearity at California soil sites during the two events was primarily manifested in the range of 1 to 3 Hz. In this frequency range, the strong-motion amplification has been reduced by a factor of 1.7–2.0 compared to linear amplification.

Acknowledgments

This study was partially supported by Iowa State University. The author is indebted to W. J. Silva, who provided an extensive digital strong-motion database used in the analyses. The article benefited from insightful reviews by L. F. Bonilla and J. Bielak.

References

Beresnev, I. A., and G. M. Atkinson (1998). FINSIM: a FORTRAN program for simulating stochastic acceleration time histories from finite faults, *Seism. Res. Lett.* **69,** 27–32.

Beresnev, I. A., and G. M. Atkinson (1999). Generic finite-fault model for ground-motion prediction in eastern North America, *Bull. Seism. Soc. Am.* **89,** 608–625.

Beresnev, I. A., and G. M. Atkinson (2001). Subevent structure of large earthquakes: a ground-motion perspective, *Geophys. Res. Lett.* **28,** 53–56.

Beresnev, I. A., and G. M. Atkinson (2002). Source parameters of earthquakes in eastern and western North America based on finite-fault modeling, *Bull. Seism. Soc. Am.* **92,** no. 2, 695–710.

Beresnev, I. A., G. M. Atkinson, P. A. Johnson, and E. H. Field (1998a). Stochastic finite-fault modeling of ground motions from the 1994 Northridge, California, earthquake. II. Widespread nonlinear response at soil sites, *Bull. Seism. Soc. Am.* **88,** 1402–1410.

Beresnev, I. A., E. H. Field, K. Van Den Abeele, and P. A. Johnson (1998b). Magnitude of nonlinear sediment response in Los Angeles basin during the 1994 Northridge, California, earthquake, *Bull. Seism. Soc. Am.* **88,** 1079–1084.

Building Seismic Safety Council (1997). NEHRP recommended provisions for seismic regulations for new buildings. I. Provisions, Rept. FEMA 302, Federal Emergency Management Agency, Washington, D.C., 337 pp.

Chin, B.-H., and K. Aki (1991). Simultaneous study of the source, path, and site effects on strong ground motion during the 1989 Loma Prieta earthquake: a preliminary result on pervasive nonlinear site effects, *Bull. Seism. Soc. Am.* **81,** 1859–1884.

Cultrera, G., D. M. Boore, W. B. Joyner, and C. M. Dietel (1999). Nonlinear soil response in the vicinity of the Van Norman Complex following the 1994 Northridge, California, earthquake, *Bull. Seism. Soc. Am.* **89,** 1214–1231.

Field, E. H., and the SCEC Phase III Working Group (2000). Accounting for site effects in probabilistic seismic hazard analyses of southern California: overview of the SCEC Phase III Report, *Bull. Seism. Soc. Am.* **90,** no. 6 (suppl.), S1–S31.

Field, E. H., P. A. Johnson, I. A. Beresnev, and Y. Zeng (1997). Nonlinear ground-motion amplification by sediments during the 1994 Northridge earthquake, *Nature* **390,** 599–602.

Field, E. H., Y. Zeng, P. A. Johnson, and I. A. Beresnev (1998). Nonlinear sediment response during the 1994 Northridge earthquake: observations and finite-source simulations, *J. Geophys. Res.* **103,** 26,869–26,883.

Hartzell, S. (1998). Variability in nonlinear sediment response during the 1994 Northridge, California, earthquake, *Bull. Seism. Soc. Am.* **88,** 1426–1437.

Petersen, M. D., W. A. Bryant, C. H. Cramer, M. S. Reichle, and C. R. Real (1997). Seismic ground-motion hazard mapping incorporating site effects for Los Angeles, Orange, and Ventura counties, California: a geographical information system application, *Bull. Seism. Soc. Am.* **87,** 249–255.

Silva, W. J., N. Abrahamson, G. Toro, and C. Costantino (1997). Description and validation of the stochastic ground motion model, report submitted to Brookhaven National Laboratory, Associated Universities, Inc., Upton, New York.

Su, F., J. G. Anderson, and Y. Zeng (1998). Study of weak and strong ground motion including nonlinearity from the Northridge, California, earthquake sequence, *Bull. Seism. Soc. Am.* **88,** 1411–1425.

Department of Geological and Atmospheric Sciences
Iowa State University
253 Science I
Ames, Iowa 50011-3212
beresnev@iastate.edu

Manuscript received 12 October 2000.